**Research paper**

# Elastic lateral-torsional buckling of steel bisymmetric double-tee section beams

## Anna Barszcz[1], Marian Giżejowski[2], Malwina Pękacka[3]

**Abstract:** Elastic lateral-torsional buckling of double-tee section structural steelworks has been widely investigated with regard to the major axis bending of single structural elements as a result of certain loading conditions. No specific attention has been paid to the general formulation in which an arbitrary span load pattern was associated with unequal end moments as a result of the moment distribution between structural members of the load bearing system. A number of analytical solutions were developed on the basis of the Vlasov theory of thin-walled members. Since the accurate closed-form solutions of lateral-torsional buckling (LTB) of beams may only be obtained for simple loading and boundary conditions, more complex situations are treated nowadays by using numerical finite element methods (FEM). Analytical and numerical methods are frequently combined for the purpose of: a) verification of approximate analytical formulae or b) presentation the results in the form of multiple curve nomograms to be used in design practice. Investigations presented in this paper deal with the energy method applied to LTB of any complex loading condition of elements of simple end boundary conditions, bent about the major axis. Firstly, a brief summary of the second-order based energy equation dealt with in this paper is presented and followed by its approximate solution using the so-called refined energy method that in the case of LTB coincides with the Timoshenko's energy refinement. As a result, the LTB energy equation shape functions of twist rotation and minor axis displacement are chosen such that they cover both the symmetric and antisymmetric lateral-torsional buckling modes. The latter modes are chosen in relation to two lowest LTB eigenmodes of beams under uniform major axis bending. Finally, the explicit form of the general solution is presented as being dependent upon the dimensionless bending moment equations for symmetric and antisymmetric components, and the in-span loads. Solutions based on the present investigations are compared for selected loading conditions with those obtained in the previous studies and verified with use of the LTBeam software. Conclusions are drawn with regard to the application of obtained closed-form solutions in engineering practice.

**Keywords:** steel beam, bisymmetric H- and I-section, elastic behaviour, lateral-torsional buckling, refined energy method, solution verification

[1]DSc., PhD., Eng., Warsaw University of Technology, Faculty of Civil Engineering, Al. Armii Ludowej 16, 00-637 Warsaw, Poland, e-mail: a.barszcz@il.pw.edu.pl,, ORCID: 0000-0002-6476-227X
[2]Prof., DSc., PhD., Eng., Warsaw University of Technology, Faculty of Civil Engineering, Al. Armii Ludowej 16, 00-637 Warsaw, Poland, e-mail: m.gizejowski@il.pw.edu.pl,, ORCID: 0000-0003-0317-1764
[3]MSc., Eng., Warsaw University of Technology Graduate, Faculty of Civil Engineering, Al. Armii Ludowej 16, 00-637 Warsaw, Poland, e-mail: malwinapekacka@onet.pl

# 1. Introduction

The elastic LTB analysis is a necessary step for the practical assessment of the inelastic lateral-torsional buckling resistance of real beams, therefore it is the subject of investigations in this paper with regard to complex loading cases. Investigations related to the linear buckling analysis of I-shaped members under moment gradient were presented in [5,9,10]. The use of energy methods in buckling problems is widely studied by Trahair [25]. Possible energy approaches for the evaluation of elastic lateral-torsional buckling problems of beams were studied by many authors, the summary of which have been given by Pi et al. [22]. A way for the refinement of the classical energy approach was shown by Timoshenko and Gere [24]. There, it has been postulated that the accuracy of classical approach of solving LTB problems may be improved by making use of the minor axis bending differential equilibrium equation. Trahair [25] refers to this method to TEM (Timoshenko's Energy Method). This method was used by many authors to solve different LTB problems of bisymmetric and monosymmetric double-tee section beams, e.g. Mohri et al. [12], Bijak [1, 3]. Bijak [2] solved flexural-torsional buckling (FTB) problems of beam-columns subjected to a combination of end moments and uniformly distributed span loads over the whole length of the member. In special cases of the zero axial compressive force, Bijak's solutions coincide with those of TEM [25]. Second order differential equilibrium equations and Bubnov–Galerkin approximate method were used. The classical energy approach was used in [8] to solve elastic flexural-torsional problems of beam-columns subjected to load patterns dependent upon a single load parameter that is able to represent the loads of the same nature but of different values in both half-lengths of the member. The general solution has been obtained by treating any arbitrary loading pattern as a superposition of symmetric and antisymmetric components, therefore the bending moment diagram is also the superposition of symmetric and antisymmetric components.

This paper is a continuation of ongoing research carried out at the Warsaw University of Technology [8]. Hence, the energy method presented in this paper for solving elastic LTB problems maintains the above mentioned superposition principle. More general energy equation is derived that accounts for the ratio of minor axis to major axis second moments of inertia. Minor axis equilibrium equation is used for the evaluation of the second derivative of the minor axis field displacements in order to replace the energy term dependent upon the product of multiplication of the mean twist rotation $\phi$ and the minor axis curvature $v''$ of the out-of-plane displacement state by the term dependent upon the twist rotation $\phi$. Since the mixed term of the higher order derivative of minor axis displacement is replaced by the twist rotation, the accuracy of the classical energy method used in [8] is improved. The proposed approach is referred hereafter to the refined energy method.

# 2. Elastic lateral-torsional buckling formulation

Let us consider a case of the elastic lateral-torsional buckling of simply supported bisymmetric double-tee section beam subjected to a nonlinear in-plane moment gradient being produced by the action effects of unequal end moments and span loads composed

of "$i$" distributed load components and "$j$" concentrated load components. The in-plane distributed load component $q_{z,i}$ acts in the range from $x_{q1,i}$ to $x_{q2,i}$ of the member length, and at the distance $z_{q,i}$ for the section shear centre, while the in-plane concentrated force $Q_{z,j}$ acts at the distance $x_{Q,j}$ from the member axis origin, and at the distance $z_{Q,j}$ from the section shear centre (Fig. 1).
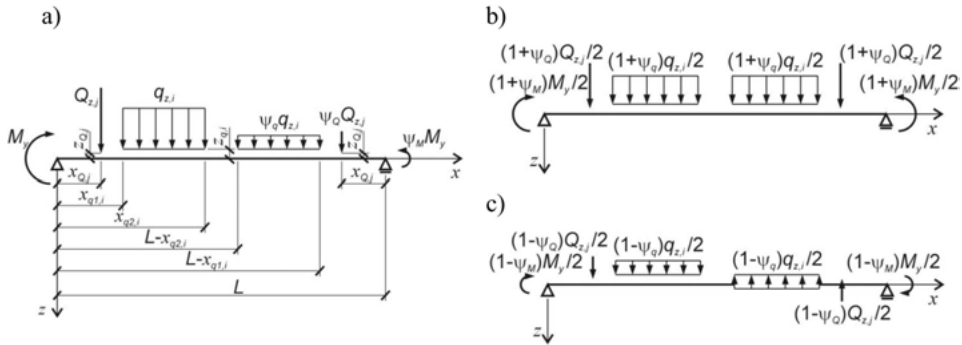


Fig. 1. Loading pattern and boundary conditions; a) general layout, b) symmetric loading pattern component; c) antisymmetric loading pattern component

The non-classical energy equation presented hereafter is formulated within the framework of linear bucking analysis (LBA) in order to formulate the equilibrium at the bifurcation state on the elastic primary equilibrium path. The developed formulation leads to the nonlinear eigenproblem analysis (NEA) that is compared to that of the linear eigenproblem analysis (LEA) presented in [8]. The Cartesian coordinate system used hereafter is that following the right hand rule.

## 2.1. Displacement field equation and displacement field derivatives

The starting point for the energy formulation is first to establish the displacement field of a thin-walled element of seven degrees of freedom. The formulation conforms to the Vlasov theory that combines the theories of Euler–Bernoulli bending and Saint Venant torsion by allowing for the warping effect. The following matrix displacement field relationship of thin-walled members holds:

(2.1)
$$\begin{bmatrix} u \\ v \\ w \end{bmatrix} = R \begin{bmatrix} \Delta s \\ y \\ z \end{bmatrix} - \begin{bmatrix} \left(1 + \omega \kappa'_x\right) \Delta x \\ y \\ z \end{bmatrix}$$

where: $R$ – space rotation matrix of the principal sectional axes of the Cartesian coordinate system, determined by considering the movement of origin and the rotation of axes $(x, y, z)$ by an angle $\varphi = \sqrt{\theta^2 + \phi^2}$ about an arbitrary axis passing through the origin ($\theta = \sqrt{\theta_y^2 + \theta_z^2}$, where $\theta_y$ and $\theta_z$ flexural rotations about the section principal axes), $\Delta s$ – member elemental

length in the displaced configuration, $\kappa_x = \kappa'_x \Delta x$ – twist [note that $(\ldots)' = \dfrac{\mathrm{d}}{\mathrm{d}x}(\ldots)$], $\omega$ – warping constant.

In the following, the deformation state variables dependent upon the $x$-coordinate. The deflected position of a double-tee section in relation to the out-of-plane buckling problems considered hereafter is defined by the prebuckling axial extension $(1 + u'_0)\,\Delta x$ and in-plane displacement $w$, as well as the postbuckling displacement $v$ and twist rotation $\theta_x$. Fig. 2 shows the deformation state of the member elemental length $\Delta x$ that translates along the coordinates $x, y, z$ ($u_0, v_0, w_0$ respectively), then develops the members axis extension $u'_0$ and rotation about the angle $\theta$.
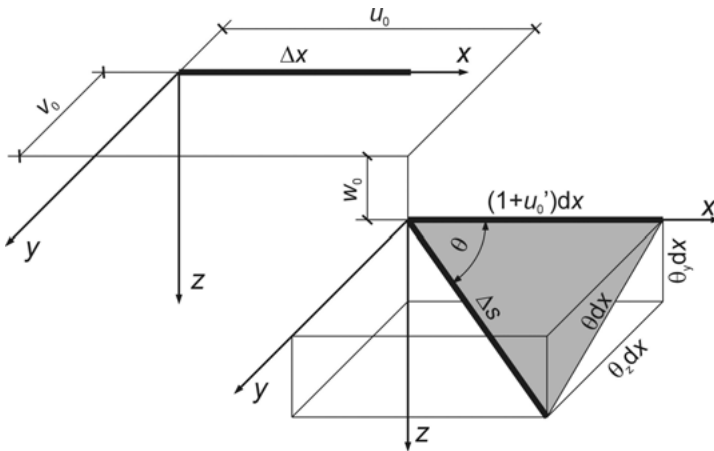


Fig. 2. Deformation state of the member elemental length $\Delta x$

The accurate rotation matrix $\boldsymbol{R}$ has been studied by Pi and Trahair [20, 21] and by Pi and Bradford [18, 19]. For the purpose of the following investigations, let us assume small rotations, i.e. $\cos\theta = 1 - \dfrac{1}{2}\theta^2$ and $\lambda = \dfrac{1}{1 + \cos\theta} = \dfrac{1}{2}$. The rotation matrix derived in the latter study [18, 19] may therefore be approximated by a sum of two components, one related to the twist rotation and the second one to the flexural rotations of the twisted section:

$$
\boldsymbol{R} = \begin{bmatrix} 1 & 0 & 0 \\ 0 & \cos\theta_x & -\sin\theta_x \\ 0 & \sin\theta_x & \cos\theta_x \end{bmatrix}
$$

$$
+ \begin{bmatrix} -\dfrac{1}{2}\theta^2 & \theta_y\sin\theta_x - \theta_z\cos\theta_x & \theta_y\cos\theta_x + \theta_z\sin\theta_x \\[2mm] \theta_z & \dfrac{1}{2}\theta_y\theta_z\sin\theta_x - \dfrac{1}{2}\theta_z^2\cos\theta_x & \dfrac{1}{2}\theta_z^2\sin\theta_x + \dfrac{1}{2}\theta_y\boxed{\theta_z}\cos\theta_x \\[2mm] -\theta_y & \dfrac{1}{2}\theta_z\boxed{\theta_y}\cos\theta_x - \dfrac{1}{2}\theta_y^2\sin\theta_x & -\dfrac{1}{2}\theta_y^2\cos\theta_x - \dfrac{1}{2}\theta_z\theta_y\sin\theta_x \end{bmatrix}
$$

where: $\theta_x$ – twist rotation about the member axis (terms being framed are the direction cosines of the section rotated about $y - y$ and $z - z$ axes, with respect to the fixed coordinate

axes of the member elemental length $\Delta x$); $\theta_y$ and $\theta_z$ – flexural rotations about the section principal axes being approximated by:

$$\theta_z = v'_0 \qquad \theta_y = -w'_0$$

The sign minus of the rotation $\theta_y$ follows from the right hand rule and terms being framed are treated as constants when differentiating the $R$ matrix. Assuming the approximations $\sin \theta_x = \theta_x$ and $\cos \theta_x = 1 - \frac{1}{2}\theta_x^2$, except for the first row of the $R$ matrix, and neglecting terms of higher than order 2, the rotation matrix of the deformable member may be expressed in the nonlinear form:

$$
R = \begin{bmatrix} 1 & 0 & 0 \\ 0 & 1 - \frac{1}{2}\theta_x^2 & -\theta_x \\ 0 & \theta_x & 1 - \frac{1}{2}\theta_x^2 \end{bmatrix} + \begin{bmatrix} -\frac{1}{2}\theta^2 & \theta_y \sin\theta_x - \theta_z \cos\theta_x & \theta_y \cos\theta_x + \theta_z \sin\theta_x \\ \theta_z & -\frac{1}{2}\theta_z^2 & \frac{1}{2}\theta_y \boxed{\theta_z} \\ -\theta_y & \frac{1}{2}\theta_z \boxed{\theta_y} & -\frac{1}{2}\theta_y^2 \end{bmatrix}
$$

Furthermore, replacing the twist rotation by its mean value $\phi$ that satisfies the following relationship:

$$\phi + \theta_x = R(3,2) - R(2,3) = 2\theta_x + \frac{1}{2}\left(\theta_z\boxed{\theta_y} - \theta_y\boxed{\theta_z}\right)$$

and considering $\Delta s = \Delta x \sqrt{1 + 2e} \approx \Delta x (1 + e)$, $e = u' + \frac{1}{2}\theta^2$, Eq. (2.1) is approximated by:

$$\begin{bmatrix} u \\ v \\ w \end{bmatrix} = R \begin{bmatrix} \Delta x \\ y \\ z \end{bmatrix} - \begin{bmatrix} \left(1 + \omega \kappa'_x\right)\Delta x \\ y \\ z \end{bmatrix}$$

where:

$$
R = \begin{bmatrix} \left(1 - \frac{1}{2}\left(\theta_y^2 + \theta_z^2\right)\right)(1 + e) & \theta_y \sin\phi - \theta_z \cos\phi & \theta_y \cos\phi + \theta_z \sin\phi \\ \theta_z(1 + e) & 1 - \frac{1}{2}\left(\phi^2 + \theta_z^2\right) & -\phi \\ -\theta_y(1 + e) & \phi & 1 - \frac{1}{2}\left(\phi^2 + \theta_y^2\right) \end{bmatrix}
$$

Hence, from the above relationship, different forms of the second order displacement field equations may be derived like those shown in the subject literature, e.g. Roik [23], Pi et al. [22], Mohri et al. [12], among others. The relationship used hereafter is of the following form:

$$\begin{bmatrix} u \\ v \\ w \end{bmatrix} = \begin{bmatrix} u_0 - \omega\kappa_x \\ v_0 \\ w_0 \end{bmatrix} + \begin{bmatrix} theta_y \sin\phi - \theta_z \cos\phi & \theta_y \cos\phi + \theta_z \sin\phi \\ -\frac{1}{2}\phi^2 & -\phi \\ \phi & -\frac{1}{2}\phi^2 \end{bmatrix} \begin{bmatrix} y \\ z \end{bmatrix}$$

The above relationship is a starting point for the evaluation of Green strain tensor components in the displaced configuration of a thin-walled member by evaluating the following derivative:

$$
\frac{\partial}{\partial x}\begin{bmatrix} u \\ v \\ w \end{bmatrix} = \frac{\partial}{\partial x}\begin{bmatrix} u_0 - \omega\kappa_x \\ v_0 \\ w_0 \end{bmatrix} + \frac{\partial}{\partial x}\begin{bmatrix} \theta_y\sin\phi - \theta_z\cos\phi & \theta_y\cos\phi + \theta_z\sin\phi \\ -\frac{1}{2}\phi^2 & -\phi \\ \phi & -\frac{1}{2}\phi^2 \end{bmatrix}\begin{bmatrix} y \\ z \end{bmatrix}
$$

$$
= \begin{bmatrix} u_0' - \omega\kappa_x' \\ \theta_z \\ -\theta_y \end{bmatrix} + \begin{bmatrix} -\kappa_z + \theta_y\kappa_x & \kappa_y + \theta_z\kappa_x \\ 0 & -\kappa_x \\ \kappa_x & 0 \end{bmatrix}\begin{bmatrix} y \\ z \end{bmatrix}
$$

where: the expressions for twist $\kappa_x$ as well as the flexural curvatures $\kappa_y$, $\kappa_z$ and the twist curvature $\kappa_x'$ are given by:

$$
\kappa_x = \phi'
$$
$$
\kappa_y = \theta_y'\cos\phi + \theta_z'\sin\phi = -\left(w_0''\cos\phi - v_0''\sin\phi\right)
$$
$$
\kappa_z = \theta_z'\cos\phi - \theta_y'\sin\phi = v_0''\cos\phi + w_0''\sin\phi
$$

and the derivative of twist (twist curvature)

$$
\kappa_x' = \phi''
$$

## 2.2. Strain components and total potential energy equation

In the following, the energy equation formulation uses the definitions of Green strain tensor components formulated with reference made to the coordinate system fixed in the undeflected position. The Green nonzero normal strain component is composed of linear and nonlinear terms, respectively $\varepsilon_{xx,L}$ and $\varepsilon_{xx,NL}$, where the latter one represents the bowing effect:

$$
\varepsilon_{xx} = \varepsilon_{xx,L} + \varepsilon_{xx,NL}
$$
$$
\varepsilon_{xx} = \frac{\partial u}{\partial x} + \frac{1}{2}\left[\left(\frac{\partial u}{\partial x}\right)^2 + \left(\frac{\partial v}{\partial x}\right)^2 + \left(\frac{\partial w}{\partial x}\right)^2\right] \approx \frac{\partial u}{\partial x} + \frac{1}{2}\left[\left(\frac{\partial v}{\partial x}\right)^2 + \left(\frac{\partial w}{\partial x}\right)^2\right]
$$

Hence

$$
\varepsilon_{xx} = u_0' - y\left(\kappa_z + \theta_y\kappa_x\right) + z\left(\kappa_y + \theta_z\kappa_x\right) - \omega\kappa_x'
$$
$$
+ \frac{1}{2}\left[\theta^2 - 2\left(y\theta_y + z\theta_z\right)\kappa_x + \left(y^2 + z^2\right)\kappa_x^2\right]
$$
$$
= u_0' - y\kappa_z + z\kappa_y - \omega\kappa_x' + \frac{1}{2}\left[\theta^2 + i_0^2\kappa_x^2\right]
$$

and

$$\varepsilon_{xx,L} = u_0' - y\kappa_z + z\kappa_y - \omega\kappa_x'$$

$$\varepsilon_{xx,NL} = \frac{1}{2}\left[\theta^2 + i_0^2\kappa_x^2\right]$$

The Green nonzero shear strain components:

$$\varepsilon_{xy,L} = \frac{\partial u(x,y,z)}{\partial y} + \frac{\partial v(x,y,z)}{\partial x} = -\frac{1}{2}\left(z + \frac{\partial \omega}{\partial y}\right)\kappa_x$$

$$\varepsilon_{xz,L} = \frac{\partial u(x,y,z)}{\partial z} + \frac{\partial w(x,y,z)}{\partial x} = \frac{1}{2}\left(y - \frac{\partial \omega}{\partial y}\right)\kappa_x$$

The obtained form of the strain field is consistent with that used by Mohri et al. [12] provided that the mean twist is approximated by the first derivative of the angle of twist rotation. The strain components are those of Pi and Bradford [18, 19] in their finite element formulation of nonlinear buckling analysis (NBA) of thin-walled members provided that coupling between the membrane and flexural states is neglected. It is worthy to notice that only one Saint Venant shear strain component is used in [18, 19], namely $\gamma = \sqrt{\varepsilon_{xy,L}^2 + \varepsilon_{xz,L}^2} = -2\rho\kappa_x$, when it is defined along the cross section mid-thickness contour line, instead of those $\varepsilon_{xy}$ and $\varepsilon_{xz}$ in the present study (where $\rho$ is the wall thickness $t$ dependent coordinate measured from the mid-thickness line and ranging from $-t/2$ to $t/2$).

As a result, the total potential energy formulation yields the sum of the strain energy $U$ and the negative work of applied loads $V$, while $U$ is the sum of $U_L$ (based on the linear terms of Green strain components) and $U_{NL}$ (based on the nonlinear term of the Green normal strain component):

$$\Pi = U_L + U_{NL} - V$$

where:

$U_L = \dfrac{1}{2}\displaystyle\int \left\{E\varepsilon_{xx,L}^2 + G\left[\varepsilon_{xy,L}^2 + \varepsilon_{xz,L}^2\right]\right\}\mathrm{d}x\,\mathrm{d}y\,\mathrm{d}z$ – strain energy based on the linear part of Green strain tensor components,

$U_{NL} = \displaystyle\int \sigma_{xx}\varepsilon_{xx,NL}\,\mathrm{d}x\,\mathrm{d}y\,\mathrm{d}z$ – initial stress work,

$V = \displaystyle\sum_i \int_{x_{q1,i}}^{x_{q2,i}} \left\{q_{y,i}\,v_i + q_{z,i}\,w_i\right\}\mathrm{d}x + \sum_j \left\{Q_{y,j}\,v_j + Q_{z,j}\,w_j\right\}$ – work done by applied

transverse distributed $q_{y,i}$, $q_{z,i}$ and concentrated $Q_{y,j}$, $Q_{z,j}$ loads.

Let us consider the LTB buckling case of in-plane transverse loads imposing the in-plane bending (major axis bending without the axial force) and neglect the terms of higher order then 2 in relation to the postbuckling out-of-plane deformation state components. Carrying out the required calculations for the out-of-plane linear buckling analysis (LBA), the total potential energy equation involving all the most important terms affecting the

member buckling state is given by:

$$
U_L = \frac{1}{2} \int_0^L \Big[ EI_z \left( v_0'' \right)^2 - \left( 1 - I_z/I_y \right) EI_y w_0'' \phi \left( 2v_0'' + w_0'' \phi \right)
$$

$$
+ \; EI_w \left( \kappa_x' \right)^2 + GI_T \left( \kappa_x \right)^2 \Big] \, dx
$$

(2.2)

$$
U_{NL} = 0
$$

$$
V = -\frac{1}{2} \left( \sum_i z_{q,i} \int_{x_{q1,i}}^{x_{q2,i}} q_{z,i} \phi_i^2 \, dx + \sum_j Q_{z,j} \, z_{Q,j} \phi_j^2 \right)
$$

The multiplier $\left( 1 - I_z/I_y \right)$ accounts for the effect of prebuckling in-plane flexural displacements on the out-of-plane buckling, and it has been denoted $k_1$ in Mohri et al. [12]. When $1 - I_z/I_y = k_1$ is replaced by unity, one obtains the classical form of the energy equation. The factor $k_1$ may be taken as equal to unity only for narrow flange I-section members for which $I_z \ll I_y$. For wide flange H-sections, the above said coefficient has to be retained for more economic design. In the following, the factor $k_1$ is consistently kept on in order to obtain the analytical solution valid for any proportion between the minor axis and major axis sectional moments of inertia. Moreover, it has to be noticed that for $I_z = I_y$ the lateral-torsional form of buckling is not possible.

## 3. General solution of the LTB problem

Let us consider the following definition of the major axis curvature at the buckling position, identified by the second derivative of the prebuckling displacement component $w_0$:

(3.1)
$$
M_y = -EI_y w_0'' \rightarrow w_0'' = -\frac{M_y}{EI_y}
$$

The minor axis curvature is obtained from the minor axis differential equilibrium equation:

(3.2)
$$
EI_z v_0'' = -M_y \phi \rightarrow v_0'' = -\frac{M_y \phi}{EI_z}
$$

On the other hand, the definition of the minor axis moment at buckling yields:

(3.3)
$$
M_y \phi = EI_z w_0'' \phi \rightarrow w_0'' \phi = \frac{M_y \phi}{EI_z}
$$

Substituting Eqs. (3.1)–(3.3) to the energy equation developed in the previous section, cf. Eq. (2.2), and performing the first variation of the resultant equation, provides a basis

for the eigenproblem formulation of the LTB problem:

$$
\frac{1}{2} \int_0^L \left\{ EI_z \delta \left[ (v_0'')^2 \right] + EI_w \delta \left[ (\phi'')^2 \right] + GI_T \delta \left[ (\phi')^2 \right] - k_1 \frac{M_y^2}{EI_z} \delta(\phi^2) \right\} \, dx
$$

$$
+ \frac{1}{2} \sum_i \int_{x_{q1,i}}^{x_{q2,i}} q_{z,i} z_{q,i} \delta \left( \phi^2 \right) dx + \frac{1}{2} \sum_j Q_{z,j} z_{Q,j} \delta \left\{ \left[ \phi \left( x_{Q,j} \right) \right]^2 \right\} = 0
$$

In the following, beams with simple member natural boundary conditions are dealt with. The buckling modes, approximating the out-of-plane displacements and twist rotations are well known trigonometric functions that satisfy boundary kinematic conditions:

$$
v = a_1 \sin(\pi\xi) + a_2 \sin(2\pi\xi)
$$

$$
\phi = a_3 \sin(\pi\xi)
$$

where: $\xi$ – dimensionless coordinate equal to $x/L$, $a_1$, $a_2$ and $a_3$ – unknown buckled shape constants.

Carrying out the variation and substituting the above cited shape functions results in the following relationship for QEA (quadratic eigenproblem analysis):

$$
\delta a^T K_{op} a = \delta a^T \left( K + \alpha_{cr} K_{\sigma,L} + \alpha_{cr}^2 K_{\sigma,NL} \right) a = 0
$$

where: $a$ – vector of the unknown buckled shape constants ($a^T = \{a_1 \ a_2 \ a_3\}$ is the $a$ vector transposed), $K_{op}$ – out-of-plane stability stiffness matrix being the sum of the constitutive component $K$, the initial stress components $K_{\sigma,L}$ and the initial displacement component $K_{\sigma,NL}$, the latter two dependent, respectively, linearly upon the reference values of in-plane loads $q_{z0,i}$ and $Q_{z0,j}$, and quadratically upon the reference value of a prebuckling stress resultant $M_{y0}$, $\alpha_{cr}$ – critical load factor.

The stiffness matrix components are of the following form:

– component $K$:

$$
K = \begin{bmatrix}
\dfrac{\pi^4 EI_z}{L^3} \displaystyle\int_0^1 \sin^2 \pi\xi \, d\xi & 0 & 0 \\[4ex]
symm. & \dfrac{16\pi^4 EI_z}{L^3} \displaystyle\int_0^1 \sin^2 2\pi\xi \, d\xi & 0 \\[4ex]
symm. & symm. & \dfrac{\pi^4 EI_w}{L^3} \displaystyle\int_0^1 \sin^2 \pi\xi \, d\xi + \dfrac{\pi^2 GI_T}{L} \displaystyle\int_0^1 \cos^2 \pi\xi \, d\xi
\end{bmatrix}
$$

– component $K_{\sigma,L}$:

$$K_{\sigma,L} = \begin{bmatrix} 0 & 0 & 0 \\ symm. & 0 & 0 \\ symm. & symm. & L\left( \sum_i \int\limits_{\xi_{q1,i}}^{\xi_{q2,i}} q_{z0,i} z_{q,i} \sin^2 \pi\xi \, d\xi + \sum_j Q_{z0,j} z_{Q,j} \sin^2 \pi\xi_j \right) \end{bmatrix}$$

– component $K_{\sigma,NL}$:

$$K_{\sigma,NL} = \begin{bmatrix} 0 & 0 & 0 \\ symm. & 0 & 0 \\ symm. & symm. & -\dfrac{(M_{y0,\max})^2 L}{EI_z} \int\limits_0^1 (m_y)^2 \sin^2 \pi\xi \, d\xi \end{bmatrix}$$

where:

$$m_y = M_{y0}/M_{y0,\max}.$$

All the stiffness matrix components are of a diagonal form, therefore the determinant of $K_{op}$ matrix is obtained by the multiplication of its diagonal terms and the buckling eigenvalue criterion becomes:

$$(3.4) \qquad \det K_{op} = 0 \quad \rightarrow \quad \prod_{n=1}^{n=3} K_{op}(n,n) = 0$$

The terms $K_{op}(n,n)$ for $n = 1, 2$ are the constant positive values, therefore only the third term contributes. As a result, the following relationship is obtained for the transverse loads applied at the shear centre:

$$(3.5) \qquad i_0^2 N_T N_z = \left( \sqrt{k_1} M_{y,\max} \right)^2 \left[ \left( \frac{M_{ys,\max}}{M_{y,\max}} \right)^2 2I_s + \left( \frac{M_{ya,\max}}{M_{y,\max}} \right)^2 2I_a \right]$$

where: $N_z$ – lowest minor axis flexural buckling force, $M_{ys,\max}$, $M_{ya,\max}$ – maximum absolute values of symmetric and antisymmetric moment components, scaling the elementary action field moment effects, $I_s = \int\limits_0^1 m_{ys}^2(\xi) \sin^2(\pi\xi) \, d\xi$ – symmetric moment integral, $m_{ys}(\xi) = \dfrac{M_{ys}(\xi)}{M_{ys,\max}}$, $I_a = \int\limits_0^1 m_{ya}^2(\xi) \sin^2(\pi\xi) \, d\xi$ – antisymmetric moment integral and $m_{ya}(\xi) = \dfrac{M_{ya}(\xi)}{M_{ya,\max}}$.

Regarding that the critical moment $M_{cr,0}$ for the uniform bending is $M_{cr,0} = i_0 \sqrt{N_T N_z}$, for $n$ symmetric and $m$ antisymmetric moment components, the integrals constituting the

diagonal initial displacement terms of the out-of-plane stiffness matrix $\boldsymbol{K}_{\sigma,NL}$ are the summation of $n$ integrals for symmetric moment components $M_{ys,i}(\xi)$ and $m$ integrals for antisymmetric moment components $M_{ya,j}(\xi)$. Therefore, Eq. (3.5) takes the form:

$$\left(\frac{\sqrt{k_1}M_{y,\max}}{M_{cr,0}}\right)^2\left[\left(\frac{M_{ys,\max}}{M_{y,\max}}\right)^2\sum_{i=1}^{i=n}\left(\frac{M_{ys,i,\max}}{M_{ys,\max}}\right)^2 2I_{s,i}+\left(\frac{M_{ya,\max}}{M_{y,\max}}\right)^2\sum_{j=1}^{j=m}\left(\frac{M_{ya,j,\max}}{M_{ya,\max}}\right)^2 2I_{a,j}\right]=1$$

or in the shortened form, similar to that used in Trahair et. al. [26]:

$$(3.6) \qquad \left(\frac{M_{y,\max}}{C_{bc}M_{cr,0}}\right)^2 = 1$$

Hence:

$$\frac{1}{C_{bc}}=\sqrt{k_1\left[\left(\frac{M_{ys,\max}}{M_{y,\max}}\right)^2\sum_{i=1}^{i=n}\left(\frac{M_{ys,i,\max}}{M_{ys,\max}}\right)^2 2I_{s,i}+\left(\frac{M_{ya,\max}}{M_{y,\max}}\right)^2\sum_{j=1}^{j=m}\left(\frac{M_{ya,j,\max}}{M_{ya,\max}}\right)^2 2I_{a,j}\right]}$$

or in the shortened form, by using the factors $C_{bs}$ for the conversion of $M_{ys}(\xi)$ and $C_{ba}$ for the conversion of $M_{ya}(\xi)$:

$$(3.7) \qquad \frac{1}{C_{bc}}=\sqrt{k_1\left[\left(\frac{M_{ys,\max}}{M_{y,\max}}\frac{1}{C_{bs}}\right)^2+\left(\frac{M_{ya,\max}}{M_{y,\max}}\frac{1}{C_{ba}}\right)^2\right]}$$

where: $\dfrac{1}{C_{bs}}=\sum_{i=1}^{i=n}\dfrac{M_{ys,i,\max}}{M_{ys,\max}}\dfrac{1}{C_{bs,i}}$, $\dfrac{1}{C_{bs,i}}=\sqrt{2I_{s,i}}$ and $\dfrac{1}{C_{ba}}=\sum_{j=1}^{j=m}\dfrac{M_{ya,j,\max}}{M_{ya,\max}}\dfrac{1}{C_{ba,j}}$,

$\dfrac{1}{C_{ba,j}}=\sqrt{2I_{a,j}}$ – conversion factors for the symmetric and antisymmetric moment diagram components.

One has to notice that Eq. (3.7) presented earlier in [17] had been derived by neglecting the effect of prebuckling displacements ($k_1 = 1$) and the elementary conversion factors $C_{bs}$ and $C_{ba}$ under the square root term of (3.7) were placed outside the round brackets. When span loads are applied away from the section shear centre, the term $K_{op}(3, 3)$ of the stiffness matrix $\boldsymbol{K}_{op}$ needs to include an additional term $K_{op,F}$ related to distributed and/or concentrated loads:

$$(3.8) \qquad K_{op}(3, 3) = i_0^2 N_T \frac{\pi^2}{2L} + K_{op,F}$$

where: $K_{op,F}$ – term related to applied off-shear centre loads as defined in Giżejowski et al. [8].

Substituting Eq. (3.8) to Eq. (3.4) and rearranging as it has been done earlier, Eq. (3.6) becomes of the following one:

$$\left(\frac{M_{y,\max}}{C_{bc}M_{cr,0}}\right)^2 = 1 + \zeta_F\frac{M_{ys,\max}hC_{bF}}{i_0^2 N_T}$$

or in the form of Eq. (3.7) in which for a single type of the span load:

$$\frac{1}{C_{bc}} = \sqrt{k_1 \frac{\left[\left(\frac{M_{ys,max}}{M_{y,max}}\frac{1}{C_{bs}}\right)^2 + \left(\frac{M_{ya,max}}{M_{y,max}}\frac{1}{C_{ba}}\right)^2\right]}{1 + \zeta_F \frac{M_{ys,max}hC_{bF}}{i_0^2 N_T}}}$$
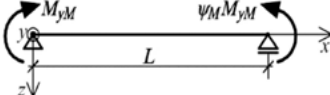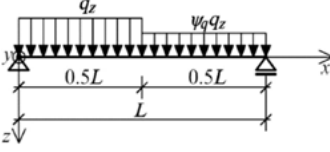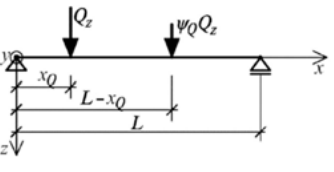
where: $C_{bF} = \frac{2L}{\pi^2}\frac{K_{op,F}}{z_F M_{ys,max}}$ – defined in Giżejowski et al. [8].

# 4. Application and verification

## 4.1. Moment conversion factors

In this subchapter, first the conversion factors $C_{bc}\sqrt{k_1}$ of present study (QEA) are compared with those obtained with use of LEA in Giżejowski et al. [8] for some important load cases dealt with. Eq. (3.7) is used to present the particular solutions for unequal end moments and for span uniformly distributed loads of unequal values in two half-lengths as well as concentrated loads of unequal values in two span half-lengths, as it is shown in Table 1. The results presented in Table 1 suggest that the differences between the LEA and QEA conversion factors in case of selected loading patterns are negligible. Moreover, QEA

Table 1. Conversion factors for simple loading cases

| Loading case | | $C_{bs}$ ($\psi_i = 1$) | | $C_{ba}$ ($\psi_i = -1$) | |
|---|---|---|---|---|---|
| $i$ | Scheme | QEA | LEA | QEA | LEA |
| M |  | 1 | 1 | 2.77 | 2.78 |
| q |  | 1.13 | 1.15 | 1.37 | 1.43 |
| Q | $x_0 = L/2$ | 1.37 | 1.42 | 0 | 0 |
| | $x_0 = L/3$ | 1.10 | 1.12 | 1.56 | 1.74 |
| | $x_0 = L/4$ | 1.04 | 1.05 | 1.73 | 1.81 |
| | $x_0 = L/6$ | 1.01 | 1.01 | 1.98 | 2.01 |
| | $x_0 = L/8$ | 1.01 | 1.01 | 2.14 | 2.15 |

results of $C_{bc}\sqrt{k_1}$ of the present study for $\psi_i = 1$ (symmetric loading cases for $i = M$, $q$, $Q$ where $q$, $Q$ are shear centre loads) conform with those of $C_{bc}\sqrt{k_1}$ in Mohri et al. [12] when the compressive force takes zero value.

In order to compare LEA and QEA solutions for combined loading patterns, authors considered the combined loading case $i = q$ "+" $M$ in the whole range of $\psi_M$ but for $\psi_q = 1$ (UDL over the entire length of the beam). The moment proportion factor $\mu$ is used being equal to the maximum moment $M_{yq} = 0.125qL^2$ for $i = q$ over the maximum moment $M_{yM}$ for $i = M$. The curves representing the conversion factor for considering uniformly distributed load and unequel end moments are presented in Fig. 3 for $\mu \leq 0$. The solid line represents the QEA solutions while the dashed line represents the LEA solutions.
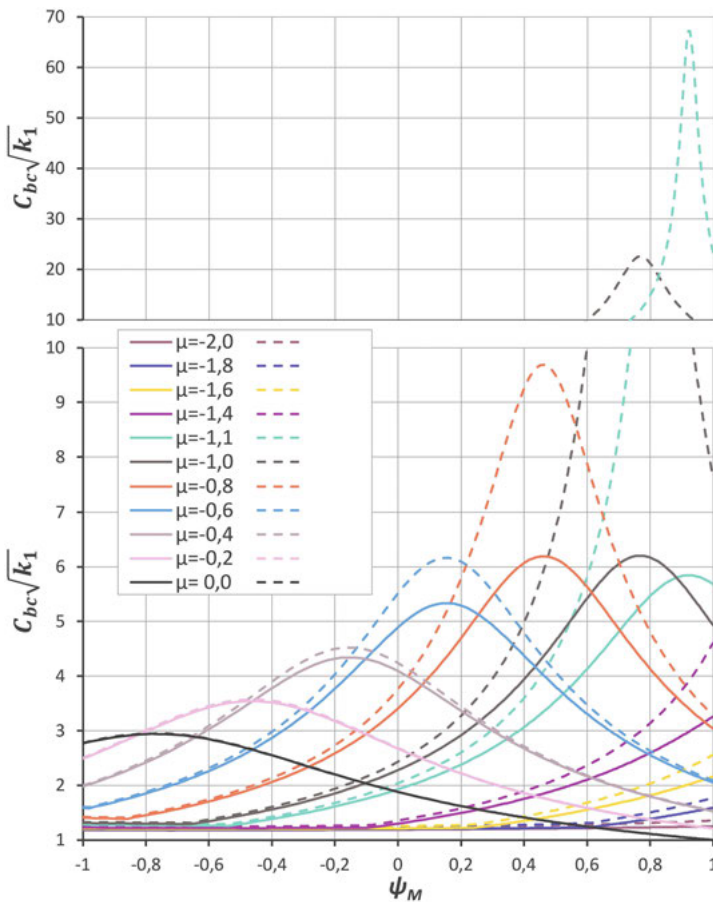


Fig. 3. Comparison of LEA and QEA conversion factors (description in the text)

Since the values of $C_{bc}\sqrt{k_1}$ in certain ranges of $\psi_M$ are distinctively apart from each other, two different scales are adopted for the ordinate axis, namely below and above $C_{bc}\sqrt{k_1} = 10$. The results prove that the difference between the LEA and QEA solutions

greatly depends upon the $\psi_M$ value. For some of the negative values of $\mu$, the $C_{bc}\sqrt{k_1}$ curves are distinctively different from each other.

The curves go up when $\psi_M$ is travelling from negative towards positive values, reaching the maximum value being greater and above those for $\psi_M = -1$. The maximum difference of $C_{bc}\sqrt{k_1}$ is reached in the range between $\mu = -0.8$ and $-1.2$. The maximum difference is observed for $\mu = -1.1$ where LEA solution reaches the maximum value of 67.4 and QEA solution reaches the maximum value of 5.84. Generally, the QEA conversion factor curves presented in this study are placed lower than those from LEA, especially for high values of $C_{bc}\sqrt{k_1}$ appearing in the range of $\mu = -0.8 \div -1.2$. The huge difference of $C_{bc}\sqrt{k_1}$ noted for an exemplary value of $\mu = -1.1$ is however for a quite unrealistic load case.

General conclusions are as follows:

1. QEA conversion factor curves presented in this study are placed lower than those of the previous LEA investigations presented in [8]. Lower values of $C_{bc}\sqrt{k_1}$ lead to the lower values of the critical moment, therefore such a conclusion is important from engineering point of view.

2. High values of $C_{bc}\sqrt{k_1}$ appear in the range of negative values of $\mu$. Noticeable differences for of $\mu$ around unity are however less important from the practical point of view since the beam buckling in the regions of high $C_{bc}\sqrt{k_1}$ appears to be elastic-plastic for steel grades used in civil engineering structures (see also Bradford et al. [4]).

3. The difference is generally lesser for the positive values of $\mu$ where it is only slightly dependent upon the value of $\psi_M$.

## 4.2. Verification for the case of combined loading

The difference in $C_{bc}\sqrt{k_1}$ values noted in the previous subsection for combined loading cases, referred mainly to the range of negative $\mu$ values need to be verified by finite element numerical simulations and other analytical solutions, especially dedicated for practical applications. In the comparison presented hereafter, design aid SN003a-EN-EU [16], supplementing the Eurocode 3, Part 1–1 [6] recommendations, is considered. Numerical simulations are performed using the finite element code LTBeam available free of cost in the public domain [11]. For calculations, a double-tee bisymmetric rolled section of IPE300 is considered for the beam of length 6 m, simply supported with regard to bending about both axes and free to warp. The following combined loading cases with unequal end moments are dealt with: $\mu = -1.0$ for UDL and $\mu = -1.2$ for CL placed at the mid-length of the beam. Figure 4 shows the results of $C_{bc}\sqrt{k_1}$.

From the presented verification exercise, the following conclusions are drawn:

1. For the considered combined loading cases, LEA solutions [8] are significantly higher than those from the other methods, either numerical made available through LTBeam code or analytical, QEA of present study and SN003a-EN-EU [16].

2. The verification exercise prove that the QEA approach presented in this study is reliable and the general solution developed in section 3 may be recommended for practical applications.

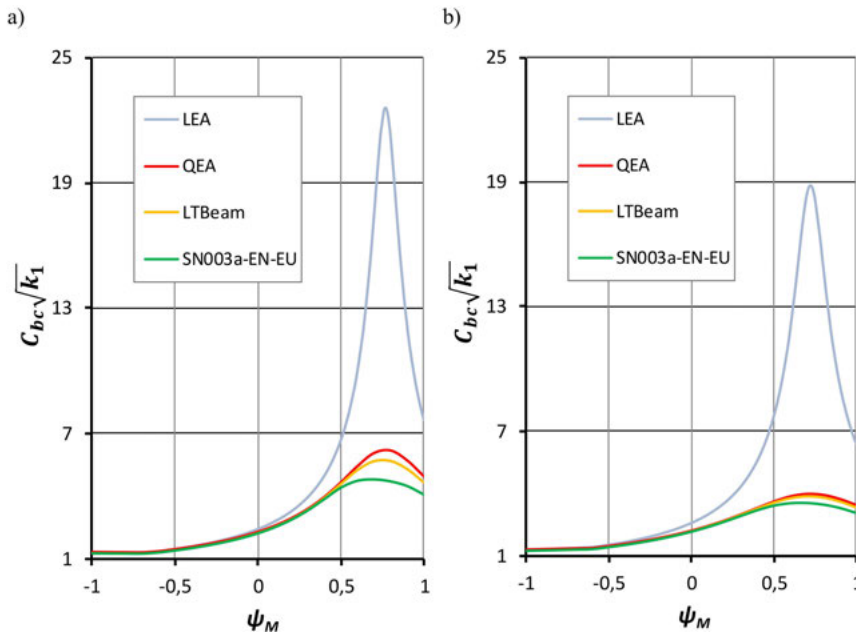a)                                              b)



Fig. 4. Comparison of the conversion factor $C_{bc}\sqrt{k_1}$ for considered combined loading cases; a) UDL and unequal end moments, b) mid-length CL and unequal end moments

3. It is worthy to notice that the lowest curve in Fig. 4 is that of SN003a-EN-EU [16]. The numerical values of $C_{bc}\sqrt{k_1}$ in the referred design aid (symbol $C_1$ is used there) were based on the conservative assumption of $I_w = 0$. This is a reason why this curve is quite close to the other curves in the range of double curvature bending while it is more conservative for the range of bending in a single curvature.

4. The general solution developed herein is valid for I and H section double-tee bisymmetric beams, through the introduction of $k_1$ factor dependent upon the minor-to-major axis moments of section inertia. Having the particular bisymmetric double-tee section, one has to calculate the $k_1$ factor, find $C_{bc}\sqrt{k_1}$ conversion factor from the diagram neglecting the effect of prebuckling displacement on the buckling state, calculate the QEA conversion factor $\left(1/\sqrt{k_1}\right)\left(C_{bc}\sqrt{k_1}\right) = C_{bc}$ that accounts for the effect of prebuckling displacements on the buckling state and finally the critical moment $M_{cr} = C_{bc}M_{cr,0}$.

In order to compare $C_1 = C_{bc}\sqrt{k_1}$ nomograms from SN003a-EN-EU [16] with those of present study, nomograms of $C_{bc}\sqrt{k_1}$ are developed with use of the QEA model of present study. Figure 5 shows the nomograms for unequal end moments and UDL in the range of $\mu \geq 0$. The solid lines represent the QEA solutions while the dashed lines reproduces the solutions from nomograms of SN003a-EN-EU [16]. Figure 6 shows the nomograms for unequal end moments and UDL in the range of $\mu \leq 0$. Figures 7 and 8 show the similar comparison for unequal end moments and mid-span CL, respectively for $\mu \geq 0$ and $\mu \leq 0$.
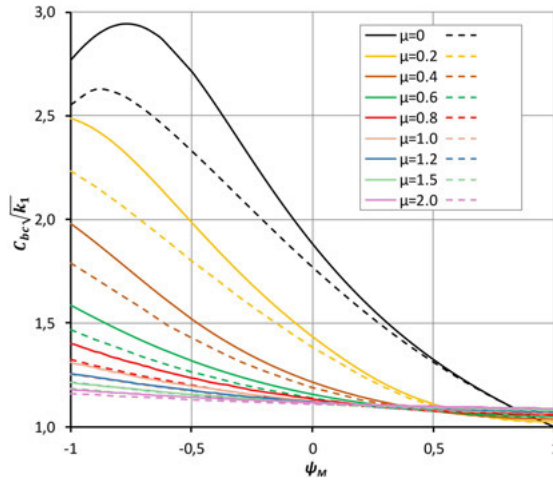
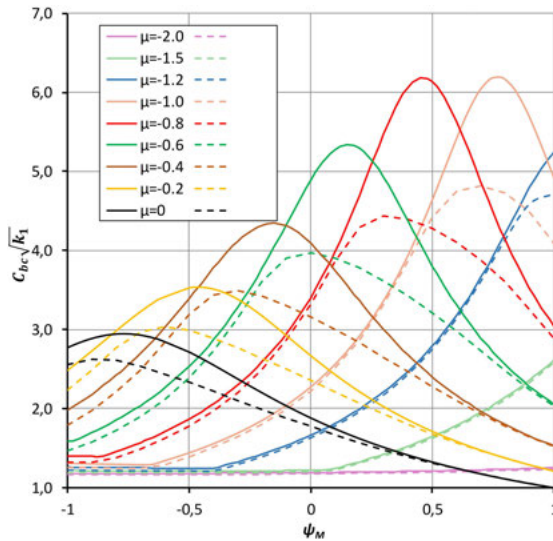Fig. 5. Nomograms of $C_{bc}\sqrt{k_1}$ for unequal end moments and UDL, and for $\mu \geq 0$



Fig. 6. Nomograms of $C_{bc}\sqrt{k_1}$ for unequal end moments and UDL, and for $\mu \leq 0$

The values of conversion factors from nomograms of SN003a-EN-EU [16] do not have fully analytical basis. They are constructed with use of the analytical solution supplemented by finite element simulations (background information has been presented in Galéa [7]). From the conducted comparison one may draw the following conclusions:

1. Nomograms developed on the basis of present study, generally coincide with those of SN003a-EN-EU [16], with a small discrepancy in the range of $C_{bc}\sqrt{k_1} = 1.5$ (discontinuity of solutions [16]).
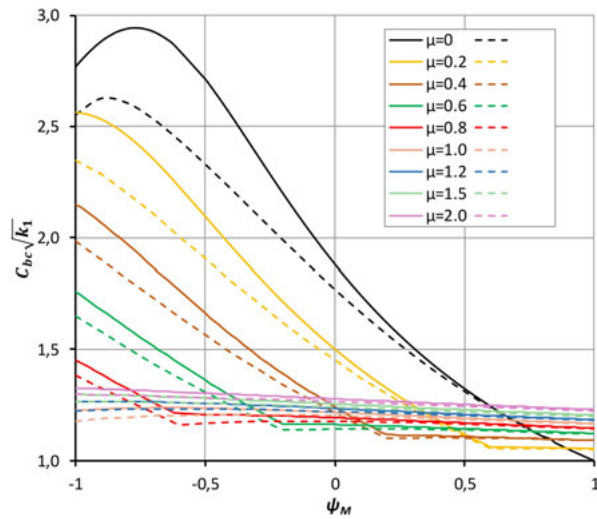
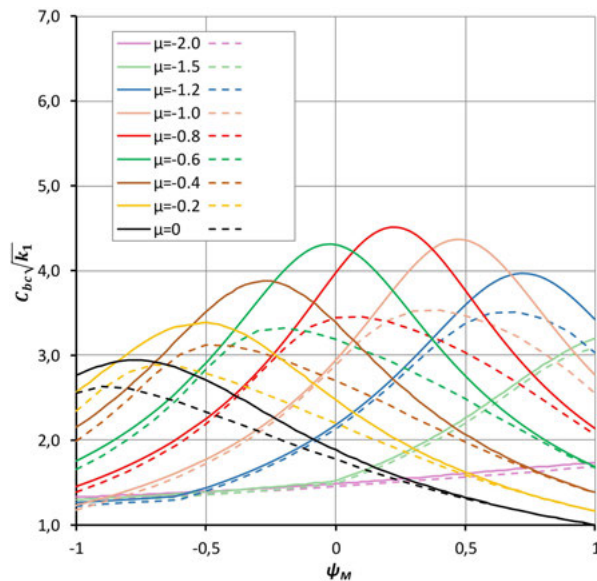Fig. 7. Nomograms of $C_{bc}\sqrt{k_1}$ for unequal end moments and CL, and for $\mu \geq 0$



Fig. 8. Nomograms of $C_{bc}\sqrt{k_1}$ for unequal end moments and CL, and for $\mu \leq 0$

2. SN003a-EN-EU nomograms [16] are placed slightly lower than those based on the present study, especially in the range of discontinuity mentioned above.

3. Despite of the predicted discrepancy, the general solution developed in the present study has the advantage of continuity, supported by fully analytical background, therefore more suitable for engineering practice. It is therefore possible to develop

a flow chart supplemented by QEA model based equations that can be easily programmed in any spreadsheet software for more suitable evaluation of the critical moment of any complex loading case.

# 5. Summary and conclusions

A nonlinear stability model for the lateral-torsional buckling of beams was presented. The formulation is based on the non-classical energy equation, presented in the form of QEA and solved analytically for any complex loading cases. The novelty of present study yields from the fact that any complex load case composed of end moments and span loads is represented by a combination of symmetric and antisymmetric components. Different loading patterns are considered as functions of load factors $\psi_M \psi_q \psi_Q$ describing the moment diagrams asymmetry under single loads of end moments as well as span UDL or CL, unequal in both half-lengths. The way of treating the loads is the same as described in [8]. Additionally, the solution includes the effect of prebuckling displacements through the section moment of inertia factor $k_1 = 1 - I_z/I_y$. Hence, the solution covers both I and H section beams of different relation between the minor and major axis moments of inertia.

Moment dependent QEA conversion factor $C_{bc}\sqrt{k_1}$ is computed using the elementary factors $C_{bs}$ (referred to the symmetric moment component) and $C_{ba}$ (referred to the antisymmetric moment component). They were compared to LEA ones developed in the authors' earlier studies. To the best authors' knowledge, QEA factors $C_{ba}$ have not yet been presented in the literature for asymmetric span loads.

More complex load cases were also dealt with on the example of unequal end moments and span UDL over the entire member length.

Conducted analyses have shown that solutions based on QEA for simple loading cases (unequal end moments and span UDL or CLs acting separately) are rather close to those based on LEA. Considering complex loading cases (unequal end moments together with shear centre span loads) it has been found that substantial differences may occur between the solutions of QEA and LEA. More important conclusion is that LEA solutions may over-predict the QEA based critical moment.

The verification exercise was carried out for complex cases of unequal end moments and span loads (UDL and mid-span CL) and a certain proportion between end moments and maximum moments produced by span loads such that giving the greatest difference between QEA and LEA solutions. In the exercise, numerical finite element results (obtained from LTBeam code) were used together with the results based on SN003a-EN-EU design aid (presented in the diagram format). It has been proven that the results from the QEA model developed in this paper coincide with those from numerical simulations and based on SN003a-EN-EU. The latter create a lower bound that is more conservative in cases giving a single in-plane bending curvature in the prebuckling state. The conservatism of SN003a-EN-EU is more visible when the beam section factor $I_z/I_y$ increase (the $k_1$ factor decrease).

# References

[1] R. Bijak, "Lateral-torsional Buckling Moment of Simply Supported Unrestrained Monosymmetric Beams", *IOP Conference Series: Materials Science and Engineering*, 2019, vol. 471, pp. 1–8, DOI: 10.1088/1757-899X/471/3/032074.

[2] R. Bijak, "Lateral-Torsional Buckling of Simply Supported Bisymmetric Beam-Columns", *Journal of Civil Engineering, Environment and Architecture*, 2017, vol. 64(3I), pp. 461–470 (in Polish), DOI: 10.7862/rb.2017.138.

[3] R. Bijak, "The Lateral Buckling of Simply Supported Unrestrained Bisymetric I-Shape Beams", *Archives of Civil Engineering*, 2015, vol. 61, no. 4, pp. 127–140, DOI: 10.1515/ace-2015-0040.

[4] M.A. Bradford, P.E. Cuk, M.A. Gizejowski, N.S. Trahair, "Inelastic lateral-buckling of beam-columns", *Journal of Structural Engineering*, 1987, vol. 113, no. 11, pp. 2259–2277.

[5] P.E. Cuk, N.S. Trahair, "Elastic buckling of beam-columns with unequal end moments", *Civil Engineering Transactions*, Institution of Engineers, Australia, 1981, vol. 3, pp. 166–171.

[6] EN 1993-1-1: 2005 *Eurocode 3: Design of Steel Structures, Part 1–1: General rules and rules for buildings*. CEN, Brussels, 2005.

[7] Y.Galéa, "Déversement élastique d'une poutre à section bi-symétrique soumise à des moments d'extrémité et une charge répartie ou concentrée", *Revue Construction Métallique*, 2002, vol. 2, pp. 59–83 (in French).

[8] M.A. Giżejowski, A.M. Barszcz, Z. Stachura, "Elastic flexural-torsional buckling of steel I-section members unrestrained between end supports", *Archives of Civil Engineering*, 2021, vol. 67, no. 1, 2021, pp. 635–656, DOI: 10.24425/ace.2021.136494.

[9] M.A. Gizejowski, Z. Stachura, J. Uziak, "Elastic flexural-torsional buckling of beams and beam-columns as a basis for stability design of members with discrete rigid restraints", in *Insights and Innovations in Structural Engineering, Mechanics and Computation*, A. Zingoni, Ed. London; Taylor & Francis Group, 2016, pp. 738–744 (e-book on CD).

[10] M.A. Gizejowski, J. Uziak, "On elastic buckling of bisymmetric H-section steel elements under bending and compression", in *Advances in Engineering Materials, Structures and Systems: Innovations, Mechanics and Applications*, A. Zingoni, Ed. London: Taylor & Francis Group, 2019, pp. 1160–1167 (e-book on CD).

[11] LTBeam. Lateral Torsional Buckling of Beams by Ivan Galéa, CTICM, 2002, https://ltbeam.software.informer.com.

[12] F. Mohri, Ch. Bouzerira, M. Potier-Ferry, "Lateral buckling of thin-walled beam-column elements under combined axial and bending loads", *Thin-Walled Structures*, 2008, vol. 46, no. 3, pp. 290–302, DOI: 10.1016/j.tws.2007.07.017.

[13] F. Mohri, A. Brouki, J.C. Roth, "Theoretical and numerical stability analyses of unrestrained, monosymmetric thin-walled beams", *Journal of Contructional Steel Research*, 2003, vol. 59, pp. 63–90, DOI: 10.1016/S0143-974X(02)00007-X.

[14] F. Mohri, N. Damil, M. Potier-Ferry, "Buckling and lateral buckling interaction in thin-walled beam-column elements with mono-symmetric cross sections", *Applied Mathematical Modelling*, 2013, vol. 37, pp. 3526–3540, DOI: 10.1016/j.apm.2012.07.053.

[15] F. Mohri, M. Potier-Ferry, "Effects of load height application and prebuckling deflections on lateral buckling of thin-walled beams", *Steel Composite Structures*, 2006, vol. 6, no. 5, pp. 401–415, DOI: 10.12989/scs.2006.6.5.401.

[16] SN003a-EN-EU *NCCI: Elastic critical moment for lateral torsional buckling*. https://eurocodes.jrc.ec.europa.eu/doc/WS2008/SN003a-EN-EU.pdf.

[17] M. Pękacka, A. Barszcz, M. Giżejowski, " Calculation of the critical moment of steel beams of bisymmetric I-sections under combined loading", *Inżynieria i Budownictwo*, 2021, vol. 1-2, pp. 74–79 (in Polish).

[18] Y.L. Pi, M.A. Bradford, "Effects of approximations in analyses of beams of open thin-walled cross-section–part I: Flexural–torsional stability", *International Journal for Numerical Methods in Engineering,* 2001, vol. 51, no. 7, pp. 757–772, DOI: 10.1002/nme.155.

[19] Y.L. Pi, M.A. Bradford, "Effects of approximations in analyses of beams of open thin-walled cross-section–part II: 3-D nonlinear behaviour", *International Journal for Numerical Methods in Engineering,* 2001, vol. 51, no. 7, pp. 773–790, DOI: 10.1002/nme.156.

[20]  Y.L. Pi, N.S. Trahair, "Nonlinear inelastic analysis of steel beam-columns", *Journal of Structural Engineering*, 1994, vol. 120, no. 7, *Part I: Theory*, pp. 2041–2061, *Part II: Applications*, pp. 2062–2085.

[21]  Y.L. Pi, N.S. Trahair, "Prebuckling deflections and lateral buckling", *Journal of Structural Engineering*, 1992, vol. 118, no. 11, *Part I: Theory*, pp. 2949–2966, *Part II: Applications*, pp. 2967–2985.

[22]  Y.L. Pi, N.S. Trahair, S. Rajasekaran, "Energy Equation For Beam Lateral Buckling", *Journal of Structural Engineering*, 1992, vol. 118, pp. 1462–1479.

[23]  K. Roik, *Vorlesungen Uber Stahlbau. Grundlagen*. Berlin-Munchen-Dusseldorf: Verlag von Wilhelm Ernst & Sohn, 1978 [in German].

[24]  S.P. Timoshenko, J.M. Gere, *Theory of Elastic Stability*, 2nd ed. New York: McGraw-Hill, 1991.

[25]  N.S. Trahair, "*Flexural-torsional buckling of structures*". Boca Raton: CRC Press, 1993.

[26]  N.S. Trahair, M.A. Bradford, D.A. Nethercot, L. Gardner, *The behaviour and design of steel structures to EC3,* 2nd ed. London-New York: Taylor and Francis, 2008.

# Sprężyste zwichrzenie belek stalowych o bisymetrycznym przekroju dwuteowym

**Słowa kluczowe:** belka stalowa, przekrój dwuteowy bisymetryczny, zachowanie sprężyste, nieklasyczne równanie energii, rozwiązanie analityczne, weryfikacja

**Streszczenie:**

Dotychczasowe badania w zakresie rozpatrywania sprężystej utraty stateczności giętno-skrętnej jako liniowego zadania wartości własnych sformułowano podstawy teoretyczne umożliwiające podjęcie studiów w zakresie nieliniowego problemu wartości własnych (NEA). W artykule przedstawiono zagadnienia sprężystego zwichrzenia stalowych belek o przekrojach dwuteowych bisymetrycznych, zginanych względem osi większej bezwładności przekroju. Badania przedstawione w pracy dotyczą analitycznej metody energetycznej odniesionej do dowolnego złożonego przypadku obciążenia, który traktuje się jako superpozycję symetrycznej i antysymetrycznej części obciążenia. Wyprowadzono nieklasyczne równanie energetyczne, które uwzględnia wpływ przemieszczeń w stanie przedkrytycznym na moment krytyczny.

W pierwszej kolejności sformułowano pole przemieszczeń oraz wyrażenie na energię potencjalną na podstawie teorii prętów cienkościennych Własowa oraz równanie energetyczne problemu spręży-stego zwichrzenia belek o rozważanym przekroju. Wyrażenie dotyczące energii potencjalnej uzależniono od uśrednionego kąta skręcenia kąta $\phi$ oraz przemieszczenia $v$ w płaszczyźnie mniejszej bezwładności przekroju. Następnie, wykorzystując równanie różniczkowe zginania w płaszczyźnie mniejszej bezwładności przekroju, równanie opisujące stan bifurkacji równowagi uzależniono jedynie od kąta skręcenia $\phi$ oraz wyprowadzono macierzową reprezentuję problemu stateczności pręta w ujęciu kwadratowego problemu wartości własnych (QEA). Ostatecznie, przedstawiono jawną postać rozwiązania liniowego problemu wartości własnych zależną od symetrycznej i antysymetrycznej części momentu zginającego. Otrzymane rozwiązanie porównano z wynikami uzyskanymi w poprzednim etapie badań, w ujęciu liniowego problemu wartości własnych (LEA).

Na podstawie przeprowadzonych analiz wykazano, że rozwiązania bazujące na QEA i uzyskane w prostych przypadkach obciążenia (momenty na końcach, obciążenie przęsłowe równomiernie rozłożone, siły skupione) są zbliżone do uzyskanych na podstawie LEA. Rozważając przypadki obciążeń złożonych (momenty na końcach łącznie z obciążeniem przęsłowym) stwierdzono znaczne różnice między rozwiązaniami QEA i LEA. Przeprowadzono weryfikację rozwiązania QEA przez porównanie wyników uzyskanych dla przypadków obciążeń złożonych charakteryzujących się największymi

równicami między QEA i LEA. Weryfikację przeprowadzono z wykorzystaniem wyników nume-rycznych metodą elementów skończonych (uzyskanych z programu LTBeam) oraz nomogramów SN003a-PL-EU wykorzystywanych w eurokodowej procedurze projektowania belek nieidealnych. Stwierdzono, że opracowany model QEA jest w wypadku złożonych stanów oddziaływań zbieżny z wynikami numerycznymi oraz wynikami z nomogramów SN003a-PL-EU, które dają konserwatywną ocenę momentów krytycznych w stanach zginania wykazującego pojedynczą krzywiznę odkształ-conej osi belki w stanie przedkrytycznym. Ocena ta staje się bardziej konserwatywna, gdy wzrasta wartość iloraz przekrojowych momentów bezwładności $I_z/I_y$ (zmniejsza się wartość parametru $k_1$).